Inorganic Chemistry
Article

Inorg. Chem. **2009**, *48*, 11601–11607 **11601**
DOI: 10.1021/ic901564y

New 3D Coordination Polymers Constructed from Pillared Metal−Formate Kagomé Layers Exhibiting Spin Canting Only in the Nickel(II) Complex

Zuo-Xi Li,[†] Jiong-Peng Zhao,[†] E. C. Sañudo,[‡] Hong Ma,[†] Zhong-Da Pan,[†] Yong-Fei Zeng,[†] and Xian-He Bu*[,†]

[†]*Department of Chemistry, Nankai University, Tianjin 300071, People's Republic of China and* [‡]*Institut de Nanociència i Nanotecnologia i Departament de Química Inorgànica, Universitat de Barcelona, Diagonal 647, 08028 Barcelona, Spain*

Received August 6, 2009

Sparked by the strategy of pillared-layer MOFs, three formate coordination polymers, $\{[Ni_2(HCO_2)_3(\mathbf{L})_2](NO_3)\cdot 2H_2O\}_\infty$ (**1**), $\{[Co_2(HCO_2)_3(\mathbf{L})_2](HCO_2)\cdot 2H_2O\}_\infty$ (**2**), and $\{[Cu_2(HCO_2)_3(\mathbf{L})_2](HCO_2)\cdot 2H_2O\}_\infty$ (**3**), have been synthesized by employing the rodlike ligand 4,4′-bis(imidazol-1-yl)biphenyl (**L**) as the pillar. Structural analysis indicates that the title complexes **1**−**3** are isostructural compounds, which possess metal−formate 2D layers perpendicularly pillared by the ligand **L** to afford a 3D open framework. This is an interesting example of a Kagomé lattice based on the formate mediator. Moreover, the formate anion of this 2D Kagomé layer exhibits various bridging modes: anti-anti, syn-anti, and 3.21 modes. Their magnetic measurements reveals that only complex **1** presents the spin canting phenomenon, while its isostructural Co^{II} and Cu^{II} complexes are simply paramagnets with antiferromagnetic coupling.

Introduction

The construction of new metal-organic frameworks (MOFs) based on pillared-layer structures is currently attracting significant attention due to their structural diversities and chemical functionality through simple modification of the pillar module and layer-mediated bridges.[1] Among various 2D lattice structures,[2] the Kagomé structure, consisting of corner-sharing triangles and showing aesthetic beauty, has evoked researchers' great interest because of its interesting magnetic properties such as spin frustration, long-range antiferromagnetic ordering, and spin-canting that can result from antiferromagnetic coupling between the nearest lattice points.[3] Up to now, most magnetic investigations of Kagomé complexes have been focused on the iron jarosite $KFe_3(OH)_6(SO_4)_2$ and its analogues.[4] However, Kagomé topological coordination polymers are still scarce.[5−9] Zaworotko and co-workers reported the first crystal engineered Kagomé lattice whose lattice vertexes are occupied by a dicopper paddle wheel, in which the Cu^{II} spins within the dimer are coupled antiferromagnetically, and the bridges between these dimers are too long to allow effective magnetic coupling.[5] Gao and co-workers prepared a 3D Co^{II} compound, $Co(N_3)_2(bpg)(DMF)_{4/3}$, with a Kagomé layer, which shows both spin frustration and long-range ordering.[6] Recently, Natarajan and co-workers represented the first single-atom-bridged Kagomé layer formed by two geometrically different hexacoordinated Mn^{II} species.[7] The coexistence of trigonal-prismatic and octahedral coordination of Mn^{II} ions reduces the frustration and gives rise to spin-canted long-range

*To whom correspondence should be addressed. E-mail: buxh@nankai.edu.cn.

(1) For examples:(a) Ren, H.; Song, T. Y.; Xu, J. N.; Jing, S. B.; Yu, Y.; Zhang, P.; Zhang, L. R. *Cryst. Growth Des.* **2009**, *9*, 105. (b) Maji, T. K.; Uemura, K.; Chang, H. C.; Matsuda, R.; Kitagawa, S. *Angew. Chem., Int. Ed.* **2004**, *43*, 3269. (c) Xiao, D. R.; Wang, E. B.; An, H. Y.; Li, Y. G.; Su, Z. M.; Sun, C. Y. *Chem. Eur. J.* **2006**, *12*, 6528. (d) Maspoch, D.; Ruiz-Molina, D.; Veciana, J. *Chem. Soc. Rev.* **2007**, *36*, 770.

(2) Richter, J.; Schulenburg, J.; Honecker, A. *Quantum Magnetism*; Springer-Verlag: Berlin, 2004.

(3) (a) Papoutsakis, D.; Grohol, D.; Nocera, D. G. *J. Am. Chem. Soc.* **2002**, *124*, 2647. (b) Bartlett, B. M.; Nocera, D. G. *J. Am. Chem. Soc.* **2005**, *127*, 8985. (c) Hastings, M. B. *Phys. Rev. B* **2001**, *63*, 014413/1.

(4) For examples:(a) Frunzke, J.; Hansen, T.; Harrison, A.; Lord, J. S.; Oakley, G. S.; Visser, D.; Wills, A. S. *J. Mater. Chem.* **2001**, *11*, 179. (b) Rao, C. N. R.; Sampathkumaran, E. V.; Nagarajan, R.; Paul, G.; Behera, J. N.; Choudhury, A. *Chem. Mater.* **2004**, *16*, 1441. (c) Behera, J. N.; Paul, G.; Choudhury, A.; Rao, C. N. R. *Chem. Commun.* **2004**, 456. (d) Grohol, D.; Nocera, D. G. *J. Am. Chem. Soc.* **2002**, *124*, 2640. (e) Nocera, D. G.; Bartlett, B. M.; Grohol, D.; Papoutsakis, D.; Shores, M. P. *Chem. Eur. J.* **2004**, *10*, 3850. (f) Greedan, J. E. *J. Mater. Chem.* **2001**, *11*, 37. (g) Paul, G.; Choudhury, A.; Sampathkumaran, E. V.; Rao, C. N. R. *Angew. Chem., Int. Ed.* **2002**, *41*, 4297.

(5) Moulton, B.; Lu, J.; Hajndl, R.; Hariharan, S.; Zaworotko, M. J. *Angew. Chem., Int. Ed.* **2002**, *41*, 2821.

(6) Wang, X. Y.; Wang, L.; Wang, Z. M.; Gao, S. *J. Am. Chem. Soc.* **2006**, *128*, 674.

(7) Mahata, P.; Sen, D.; Natarajan, S. *Chem. Commun.* **2008**, 1278.

(8) Zeng, Y. F.; Hu, X.; Zhao, J. P.; Hu, B. W.; Sanudo, E. C.; Liu, F. C.; Bu, X. H. *Chem. Eur. J.* **2008**, *14*, 7127.

(9) For examples:(a) Rusanov, E. B.; Ponomarova, V. V.; Komarchuk, V. V.; Stoeckli-Evans, H.; Fernandez-Ibañez, E.; Stoeckli, F.; Sieler, J.; Domasevitch, K. V. *Angew. Chem., Int. Ed.* **2003**, *42*, 2499. (b) Perry, J. J.; McManus, G. J.; Zaworotko, M. J. *Chem. Commun.* **2004**, 2534. (c) Liu, Y. L.; Kravtsov, V. C.; Beauchamp, A.; Eubank, J. F.; Eddaoudi, M. *J. Am. Chem. Soc.* **2005**, *127*, 7266. (d) Baudron, S. A.; Batail, P.; Coulon, C.; Clérac, R.; Canadell, E.; Laukhin, V.; Melzi, R.; Wzietek, P.; Jérome, D.; Auban-Senzier, P.; Ravy, S. *J. Am. Chem. Soc.* **2005**, *127*, 11785. (e) Awaga, K.; Okuno, T.; Yamaguchi, A.; Hasegawa, M.; Inabe, T.; Maruyama, Y.; Wada, N. *Phys. Rev. B* **1994**, *49*, 3975.

Published on Web 11/30/2009

ordering behavior. Our group reported a 2D compound with an anionic Kagomé sheet based on a $[Cu_4]$ unit, which exhibits strong antiferromagnetism.[8] Additionally, other Kagomé-type networks can be also found in the literature,[9] but the design and investigation of such unique structured materials, especially those featuring magnetic properties, remains a challenge.

As the smallest carboxylate, the formate anion HCO_2^- is a versatile three-atom bridge that can effectively mediate the magnetic coupling. In comparison to other small multitopic ligands such as CN^- (cyanide),[10] N_3^- (azide),[11] and $C_2O_4^{2-}$ (oxalate),[12] the formate anion has been observed to exhibit a large variety of bridging modes such as 2.11, 3.21, and 4.22 patterns to link two or more transition-metal ions,[13] thus providing a versatile "building block" for constructing molecular magnetic materials. Thus, it would be very interesting to synthesize pillar-layer complexes based on metal−formate 2D layers. 2D topological lattices and rodlike pillars have been exploited in the engineering of pillar-layer architectures with success.[14] Usually, the magnetic properties are greatly affected by the used pillar, and thus, the pillar determines the 3D final structure and magnetism.[5,15] In light of these aspects mentioned above, herein we employed the linear ligand 4,4′-bis(imidazolyl)biphenyl (**L**) as the pillar and obtained the three isostructural compounds **1**−**3** based on the metal−formate Kagomé layer under different conditions. All of the complexes have been characterized by elemental analysis, IR, and X-ray powder diffraction, and their crystal structures have been elucidated by X-ray crystallography. The magnetic properties have also been investigated.

Experimental Section

Materials and General Procedures. All the solvents and reagents for synthesis were commercially available and used as received. Ligand **L** was synthesized according to the literature procedures.[16] Elemental analyses of C, H, and N were performed on a Perkin-Elmer 240C analyzer. IR spectra were measured on a TENSOR 27 (Bruker) FT-IR spectrometer with KBr pellets. X-ray powder diffraction (XRPD) was carried out on a Rigaku D/Max-2500 diffractometer at 40 kV, 100 mA for a Cu-target tube, and a graphite monochromator. Magnetic data were collected at the Unitat de Mesures Magnètiques at the Universitat de Barcelona using crushed crystals of the sample on a Quantum Design MPMS-XL SQUID magnetometer equipped with a 5T magnet. The diamagnetic corrections were calculated using Pascal's constants.

Syntheses of Complexes 1−3. $\{[Ni_2(HCO_2)_3(L)_2](NO_3)\cdot 2H_2O\}_\infty$ **(1).** The compound was synthesized by the solvothermal method. A suspension of $Ni(NO_3)_2\cdot 6H_2O$ (0.12 mmol, 35 mg) and **L** (0.1 mmol, 29 mg) in 10 mL of component solvent ($DMF/H_2O/C_2H_5OH$ = 4/3/3) was sealed in a Teflon-lined autoclave and heated to 140 °C for 4 days. After the autoclave was cooled to room temperature at 10 °C h^{-1}, green block crystals suitable for single-crystal X-ray crystallographic analysis were obtained. The mother liquor was decanted, and the crystals were rinsed three times with ethanol (8 mL × 3) and dried in air for 2 h (yield ca. 30% based on **L**). Anal. Calcd for $C_{39}H_{35}Ni_2N_9O_{11}$: C, 49.74; H, 3.98; N, 13.66. Found: C, 49.36; H, 4.10; N. 13.50. IR (KBr, cm^{-1}): 3137 (w), 1587 (s), 1518 (s), 1384 (m), 1348 (w), 1313 (w), 1255 (m), 1126 (w), 1064 (s), 962 (m), 825 (s), 738 (w), 655 (m), 519 (w).

$\{[Co_2(HCO_2)_3(L)_2](HCO_2)\cdot 2H_2O\}_\infty$ **(2).** Single crystals of **2** suitable for X-ray analysis were obtained by a modified method of that described above for **1**. A mixture of $Co(NO_3)_2\cdot 6H_2O$ (0.12 mmol, 35 mg) and **L** (0.1 mmol, 29 mg) was suspended in 10 mL of component solvent ($DMF/H_2O/C_2H_5OH$ = 4/3/3). After addition of 1.0 mL formic acid solution (88%), the suspension was heated in a Teflon-lined autoclave (20 mL) at 140 °C for 4 days. After the mixture was slowly cooled to room temperature, along with a small amount of powder, orange block crystals were obtained. The powder product was removed by decanting with water, and the crystals were rinsed three times with ethanol (8 mL × 3) and dried in air for 2 h (yield ca. 35% based on **L**). Anal. Calcd for $C_{40}H_{36}Co_2N_8O_{10}$: C, 48.79; H, 3.95; N, 12.36. Found: C, 48.42; H, 3.85; N, 12.21%. IR (KBr, cm^{-1}): 3133 (m), 2868 (w), 1590 (s), 1518 (s), 1346 (w), 1313 (w), 1254 (m), 1121 (m), 1063 (s), 961 (m), 939 (w), 815 (w), 739 (m), 653 (m), 518 (m).

$\{[Cu_2(HCO_2)_3(L)_2](HCO_2)\cdot 2H_2O\}_\infty$ **(3).** This compound was prepared by the layering method. A buffer layer of H_2O/C_2H_5OH (1/1, 8 mL) was carefully layered over a solution of $Cu(HCO_2)_2\cdot 2H_2O$ (11.4 mg, 0.06 mmol) in H_2O (6 mL). Then a solution of **L** (11.4 mg, 0.04 mmol) in C_2H_5OH (6 mL) was layered over the buffer layer. After ca. 4 weeks, blue prism crystals appeared at the boundary (yield ca. 25% based on **L**). Anal. Calcd for $C_{40}H_{36}Cu_2N_8O_{10}$: C, 51.63; H, 4.19; N, 11.85. Found: C, 51.04; H, 4.11; N, 11.56. IR (KBr, cm^{-1}): 3417 (s), 3136 (s), 1592 (m), 1521 (m), 1400 (s), 1316 (m), 1261 (w), 1135 (w), 1067 (w), 964 (w), 835 (w), 652 (w).

X-ray Crystallographic Measurements for 1−3. X-ray single-crystal diffraction data of these compounds were collected on a Rigaku MM-007/Saturn 70 with graphite-monochromated Mo Kα radiation (λ = 0.710 73 Å). The program SAINT[17] was used for integration of the diffraction profiles. All the structures were solved by direct methods using the SHELXS program of the SHELXTL package and refined by full-matrix least-squares methods with SHELXL.[18] Metal atoms in each complex were located from the *E* maps, and other non-hydrogen atoms except for those in the counterions were located in successive difference Fourier syntheses and refined with anisotropic thermal parameters on F^2. The hydrogen atoms of the ligands were generated theoretically onto the specific atoms and refined isotropically. The free counteranions (NO_3^- and HCO_2^-) in the three title

(10) For examples:(a) Li, D.; Parkin, S.; Wang, G.; Yee, G. T.; Clérac, R.; Wernsdorfer, W.; Holmes, S. M. *J. Am. Chem. Soc.* **2006**, *128*, 4214. (b) Ohba, M.; Kaneko, W.; Kitagawa, S.; Maeda, T.; Mito, M. *J. Am. Chem. Soc.* **2008**, *130*, 4475. (c) Ni, Z. H.; Kou, H. Z.; Zhang, L. F.; Ge, C.; Cui, A. L.; Wang, R. J.; Li, Y.; Sato, O. *Angew. Chem., Int. Ed.* **2005**, *44*, 7742.

(11) (a) Liu, T. F.; Fu, D.; Gao, S.; Zhang, Y. Z.; Sun, H. L.; Su, G.; Liu, Y. J. *J. Am. Chem. Soc.* **2003**, *125*, 13976. (b) Zeng, Y. F.; Hu, X.; Liu, F. C.; Bu, X. H. *Chem. Soc. Rev.* **2009**, *38*, 469.

(12) (a) Coronado, E.; Galán-Mascarós, J. R.; Martí-Gastaldo, C. *J. Am. Chem. Soc.* **2008**, *130*, 14987. (b) Alberola, A.; Coronado, E.; Galán-Mascarós, J. R.; Giménez-Saiz, C.; Gómez-García, C. J. *J. Am. Chem. Soc.* **2003**, *125*, 10774.

(13) (a) Wang, X. Y.; Wei, H. Y.; Wang, Z. M.; Chen, Z. D.; Gao, S. *Inorg. Chem.* **2005**, *44*, 572. (b) Harris notation: Harris notation describes the binding mode as [X·Y1Y2Y3...Yn], where X is the overall number of metals bound by the whole ligand, and each value of Y refers to the number of metal atoms attached to the different donor atoms. The ordering of Y is listed by the Cahn−Ingold−Prelog priority rules.

(14) For examples:(a) Kitaura, R.; Fujimoto, K.; Noro, S. I.; Kondo, M.; Kitagawa, S. *Angew. Chem., Int. Ed.* **2002**, *41*, 133. (b) Ma, L. F.; Wang, L. Y.; Huo, X. K.; Wang, Y. Y.; Fan, Y. T.; Wang, J. G.; Chen, S. H. *Cryst. Growth Des.* **2008**, *8*, 620. (c) Chen, Z.; Zhou, Y.; Weng, L.; Zhao, D. *Cryst. Growth Des.* **2008**, *8*, 4045. (d) Lü, J.; Shen, E.; Li, Y.; Xiao, D.; Wang, E.; Xu, L. *Cryst. Growth Des.* **2005**, *5*, 65. (e) Ruiz-Prez, C.; Lorenzo-Luis, P. A.; Hernndez-Molina, M.; Laz, M. M.; Gili, P.; Julve, M. *Cryst. Growth Des.* **2004**, *4*, 57.

(15) Rujiwatra, A.; Kepert, C. J.; Claridge, J. B.; Rosseinsky, M. J.; Kumagai, H.; Kurmoo, M. *J. Am. Chem. Soc.* **2001**, *123*, 10584.

(16) Fan, J.; Hanson, B. E. *Chem. Commun.* **2005**, 2327.

(17) Bruker A. X. S., *SAINT Software Reference Manual*, Bruker-AXS: Madison, WI, 1998.

(18) Sheldrick, G. M. *SHELXTL NT Version 5.1, Program for Solution and Refinement of Crystal Structures*; University of Göttingen, Göttingen, Germany, **1997**.

Table 1. Crystallographic Data and Structure Refinement Parameters for Compounds **1**−**3**

	1	**2**	**3**
chem formula	$C_{39}H_{35}Ni_2N_9O_{11}$	$C_{40}H_{36}Co_2N_8O_{10}$	$C_{40}H_{36}Cu_2N_8O_{10}$
formula wt	923.18	906.63	915.85
cryst syst	monoclinic	monoclinic	monoclinic
space group	$P2_1/c$	$P2_1/c$	$P2_1/c$
a (Å)	17.980(4)	17.884(4)	18.221(4)
b (Å)	11.711(2)	11.797(2)	11.985(2)
c (Å)	19.921(4)	20.243(4)	22.525(9)
β (deg)	110.97(3)	111.77(3)	115.68(2)
V (Å^3)	3917.2(14)	3966.0(14)	4433(2)
Z	4	4	4
D_{calcd} (g cm^{-3})	1.565	1.518	1.372
μ (mm^{-1})	1.036	0.906	1.022
F(000)	1904	1864	1880
no. of rflns collected/unique	28 731/6887	33 763/6948	34 071/7808
R_{int}	0.1142	0.0628	0.1439
R1[a] ($I > 2\sigma(I)$)	0.1238	0.0619	0.0964
wR2[b]	0.2921	0.1649	0.2116
GOF	1.185	1.086	1.108

[a] $R1 = \sum||F_o| - |F_c||/\sum|F_o|$. [b] $wR2 = [\sum[w(F_o^2 - F_c^2)^2]/\sum w(F_o^2)^2]^{1/2}$.

compounds **1**−**3** are disordered, and each one has been split into two parts. Further details of the structural analysis are summarized in Table 1, and selected bond lengths and angles are given in Table 2.

Results and Discussion

Synthesis Consideration and General Characterization. With the concept of pillar-layer architecture in mind, we employed a ditopic ligand, 4,4′-bis(imidazolyl)biphenyl, as the pillar to construct the three isostructural compounds **1**−**3** based on the metal−formate 2D layer. Compound **1** was synthesized under solvothermal conditions. It is worth noting that the formate anion was generated by in situ hydrolysis of DMF.[19] Under similar conditions using $Co(NO_3)_2$ instead of $Ni(NO_3)_2$, the 1-D compound $\{[Co(H_2O)_4(\mathbf{L})](\mathbf{L})_3\cdot 2NO_3\}_\infty$ (**4**), which contains no formate anion, was obtained.[20] This was probably due to the low concentration of formate. Thus, formic acid was added into the reaction system and the target compound $\{[Co_2(HCO_2)_3(\mathbf{L})_2](HCO_2)\cdot 2H_2O\}_\infty$ (**2**), isostructural with **1**, was successfully obtained ($n(HCO_2H)/n(Co^{II}) \approx 190/1$). Using the solvothermal method, only a viscous solution was obtained from the Cu reaction system. Thus, taking advantage of $Cu(HCO_2)_2$ being readily soluble in water and many polar organic solvents, e.g. CH_3OH, C_2H_5OH, and DMF, a layering method was employed at room temperature, and the isostructural compound $\{[Cu_2(HCO_2)_3(\mathbf{L})_2](HCO_2)\cdot 2H_2O\}_\infty$ (**3**) was successfully isolated. All of these show how a variety of synthetic strategies for the generation of these isostructural compounds are available and can be adapted to each particular reaction system.

In the three pillar-layered compounds, there exist free counteranions, which are disordered. Their free anions could be assigned by crystallographic analysis in spite of their disorder, which were corroborated by their IR spectra and EA. The spectra of **1** exhibit an absorption band at ~1384 cm^{-1} characteristic of free NO_3^- anions,[21] while for **2** and **3**, the ~1590 cm^{-1} peaks are consistent with the isolated HCO_2^- anions,[22]

Crystal Structures. Single-crystal X-ray diffraction analysis reveals that the three title compounds **1**−**3** are isomorphous and isostructural, and thus only the structure of **2** is presented here as an example. Compound **2** crystallizes in the monoclinic space group $P2_1/c$. The asymmetric unit consists of two crystallographically independent Co^{II} centers, three coordinating formate ions, two **L** ligands, one free formate ion, and two water molecules. Figure 1a illustrates the coordination environments of the two unique Co^{II} ions. Co1 is hexacoordinated in a distorted octahedral fashion; it is equatorially coordinated by two oxygen atoms from two anti-anti formate ions (O5−C3−O6), one oxygen atom from one syn-anti formate ion, and one oxygen atom from one 3.21 mode formate ion with Co−O distances of 2.09−2.16 Å, and the axial positions are occupied by two N atoms from two trans-coordinated **L** ligands with an average Co−N distance of 2.12 Å, forming an octahedral coordination environment. Co2 is pentacoordinated in a distorted square-pyramidal fashion. The apical position is occupied by O1 (Co2−O1 distance is 2.11 Å) from a formate bridging ligand, and the four basal positions are occupied by two N atoms from two trans-coordinated **L** ligands with a Co−N distance of 2.07 Å and two O atoms with Co−O distances of 2.06 and 2.12 Å. The coordination bond lengths and angles around the Co^{II} ion are in good agreement with those typically observed (Table 2).[23] It is worth mentioning that

Table 2. Comparison of Some Important Bond Lengths (Å) and Angles (deg) for **1**−**3**

	M = Ni^{II}	M = Co^{II}	M = Cu^{II}
M1−O2 (3.2.1)	2.098(7)	2.151(3)	**2.434(5)**
M1−O4 (syn-anti)	2.142(6)	2.162(3)	**2.470(5)**
M1−O5 (anti-anti)	2.116(8)	2.094(3)	2.096(5)
M1−O6 (anti-anti)	2.044(7)	2.086(3)	2.089(5)
M1−N5	2.078(7)	2.127(4)	2.090(6)
M1−N7	2.088(7)	2.122(4)	2.078(6)
M2−O1 (3.2.1)	2.097(8)	2.111(3)	2.071(5)
M2−O1A (3.2.1)	2.103(7)	2.124(3)	**2.418(5)**
M2−O3 (syn-anti)	2.038(10)	2.056(4)	2.073(5)
M2−O4 (syn-anti)	**2.485(8)**	**2.641(3)**	**2.774(5)**
M2−N1	2.056(7)	2.074(4)	2.036(6)
M2−N3	2.044(7)	2.068(4)	2.044(6)
M2−O1−M2A	102.9(3)	102.74(12)	101.93(19)
O1−M2−O1A	77.1(3)	77.26(12)	78.07(19)

(19) Procedure of hydrolysis: $HC(O)N(CH_3)_2 + H_2O \rightarrow HCO_2H + HN(CH_3)_2$. For examples:(a) Chen, J.; Ohba, M.; Kitagawa, S. *Chem. Lett.* **2006**, *35*, 526. (b) Hawxwell, S. M.; Brammer, L. *CrystEngComm* **2006**, *8*, 473. (c) Burrows, A. D.; Cassar, K.; Friend, R. M. W.; Mahon, M. F.; Rigby, S. P.; Warren, J. E. *CrystEngComm* **2005**, *7*, 548. (d) Chen, W.; Wang, J. Y.; Chen, C.; Yue, Q.; Yuan, H. M.; Chen, J. S.; Wang, S. N. *Inorg. Chem.* **2003**, *42*, 944.

(20) Crystallographic data of **4** are as follows: $C_{72}H_{64}CoN_{18}O_{10}$, MW = 1414.80, triclinic, $P\bar{1}$, a = 9.290(2) Å, b = 11.615(3) Å, c = 16.526(4) Å, α = 96.347(4)°, β = 96.341(4)°, γ = 105.073(4)°, V = 1693.2(7) Å^3, D_{calcd} = 1.373 g cm^{-3}, final R1 = 0.0843, wR2 = 0.2677 (for $I > 2\sigma$), GOF = 1.041, and Z = 1. Further details for structural analysis are depicted in Figure S1 (Supporting Information).

(21) (a) Amouri, H.; Guyard-Duhayon, C.; Vaissermann, J. *Inorg. Chem.* **2002**, *41*, 1397. (b) Kure, B.; Fukuzumi, S.; Ogo, S. *Chem. Lett.* **2007**, *36*, 1468.

(22) (a) Mondal, R.; Basu, T.; Sadhukhan, D.; Chattopadhyay, T.; Bhunia, M. k. *Cryst. Growth Des.* **2009**, *9*, 1095. (b) Lang, H.; Shen, Y.; Rüffer, T.; Walfort, B. *Inorg. Chim. Acta* **2008**, *361*, 95.

(23) For examples:(a) Majumder, A.; Gramlich, V.; Rosair, G. M.; Batten, S. R.; Masuda, J. D.; El Fallah, M. S.; Ribas, J.; Sutter, J. P.; Desplanches, C.; Mitra, S. *Cryst. Growth Des.* **2006**, *6*, 2355. (b) Carbonera, C.; Dei, A.; Létard, J. F.; Sangregorio, C.; Sorace, L. *Angew. Chem., Int. Ed.* **2004**, *43*, 3136. (c) Xie, C.; Zhang, B.; Liu, X.; Wang, X.; Kou, H.; Shen, G.; Shen, D. *Inorg. Chem. Commun.* **2004**, *7*, 1037. (d) Billson, T. S.; Crane, J. D.; Fox, O. D.; Heath, S. L. *Inorg. Chem. Commun.* **2000**, *3*, 718.

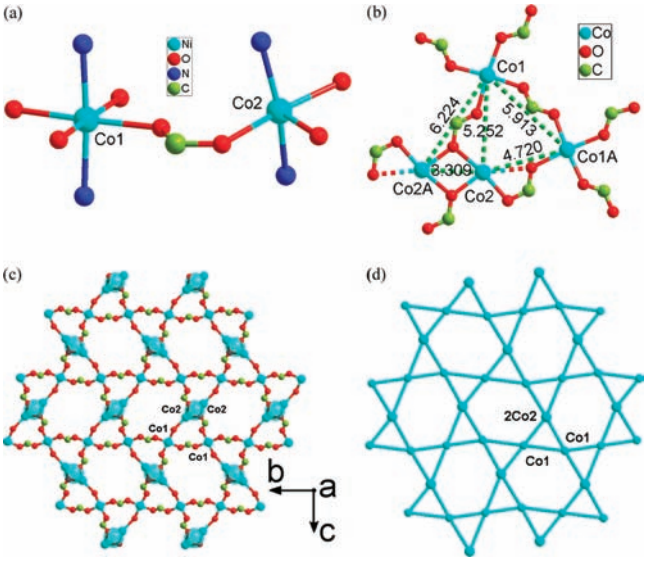

Figure 1. (a) Octahedral and square-pyramidal coordination environments of Co^{II} ions (hydrogen atoms omitted for clarity). (b) Miscellaneous bridging mode of formate anion and corresponding Co−Co connectivity. (c) Metal−formate 2D layer composed of hexagonal rings and triangular rings (atoms C2 and O3 omitted for clarity). (d) Binodal Kagomé lattice for the title 2D layer.

the Co2 center is located in a distorted square-pyramidal coordination sphere, and an unusual five-coordination of Co^{II} ion is observed in this complex.[24] As shown in Figure 1b, the formate anions show three different bridging modes: anti-anti for O5−C3−O6, syn-anti for O3−C2−O4, and 3.21 bridging mode for O1−C1−O2. Significantly, there exists a weak interaction between Co2 and O4, with a Co···O distance of 2.64 Å.[25] Owing to the diversity of bridging modes, there are five kinds of magnetic coupling pathways mediated by the formate anion, with the Co−Co distances being Co1−Co1A = 5.91 Å, Co2−Co2A = 3.31 Å, Co1A−Co2 = 4.72 Å, Co1−Co2 = 5.25 Å, and Co1−Co2A = 6.22 Å.

The formate−cobalt network is a novel intricate layer containing two unique metal centers, Co1 and Co2. Two adjacent Co2 square-base pyramids are doubly bridged by two formate oxygen atoms, and the Co···Co separation is only 3.31 Å. If the two Co2 square-base pyramids are considered as one node and meanwhile the Co1 octahedron is viewed as another node, then the 2D layer is composed of hexagonal rings delimited by six triangular rings, whereas the triangular ring rivets with three nearest neighbors and the adjacent triangles share only one lattice node, as shown in Figure 1c. Topologically, such a layer consisting of tungsten bronze sheets is the characteristic Kagomé lattice based on the heterogeneous four-connected nodes (Figure 1d). To the best of our knowledge, this is the first example of a metal−formate Kagomé layer. The planar Kagomé layer is further perpendicularly pillared by the long

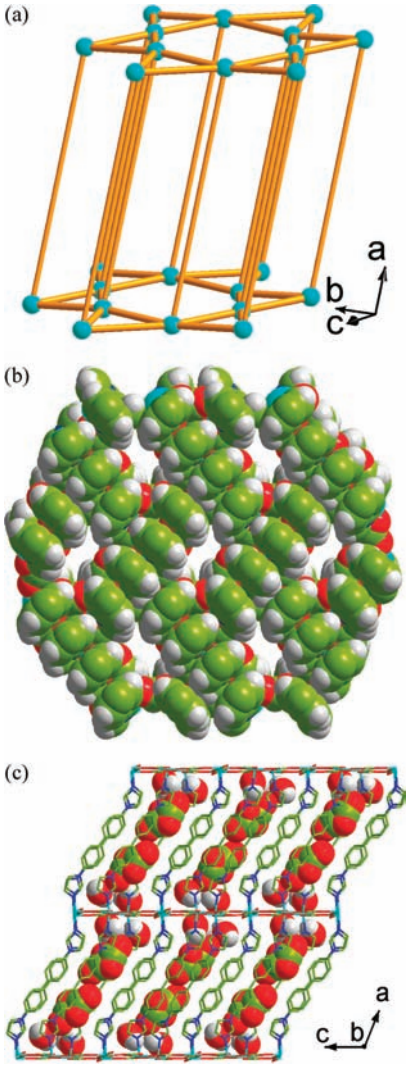

Figure 2. (a) 3D pillar-layer architecture of **2**. (b) Irregular channel built from the hexagonal ring pillared by ligand **L**. (c) Inhabited water molecules and formate anions in the channel.

linear **L** ligand to afford an extended 3D cationic framework, $[Co_2(HCO_2)_3(\mathbf{L})_2]_\infty$ (Figure 2a). Furthermore, the 2D layers are pillared in such a way that 1D hexagonal channels are obtained (Figure 2b). Unfortunately, the void space of the channels is occupied in the crystal by water molecules and free formate anions, which destroys the porosity (Figure 2c).

Complex **1** is isostructural with compound **2**, with slightly different coordination spheres for the metals. Ni1 is hexacoordinated in a distorted octahedral fashion, and the Ni2 sites (equivalent to Co2) are square-based pyramidal in geometry, but with a sixth atom (O4) in the coordination sphere of the Ni^{II}, the Ni2−O4 distance is 2.49 Å, just in the limit of being considered a coordination bond. Compound **3** is also isostructural with compound **2**, displaying the same pillared architecture but accommodating the Cu^{II} preference for being tetracoordinated. The octahedral sites occupied by Cu1 are very clearly elongated, with Cu1−O2 and Cu1−O4 distances trans to each other being 2.43 and 2.47 Å, respectively. The pentacoordinated sites display a very elongated apical Cu2−O1A bond of 2.42 Å.

(24) For examples:(a) Biswas, M.; Pilet, G.; Salah El Fallah, M.; Ribas, J.; Mitra, S. *Inorg. Chim. Acta* **2008**, *361*, 387. (b) Konarev, D. V.; Khasanov, S. S.; Saito, G.; Lyubovskaya, R. N. *Cryst. Growth Des.* **2009**, *9*, 1170. (c) Cuevas, A.; Kremer, C.; Suescun, L.; Russi, S.; Mombrú, A. W.; Lloret, F.; Julve, M.; Faus, J. *Dalton Trans.* **2007**, 5305. (d) Garoufis, A.; Kasselouri, S.; Raptopoulou, C. P. *Inorg. Chem. Commun.* **2000**, *3*, 251. (e) Kong, D.; Huang, X.; Xie, Y. *Inorg. Chim. Acta* **2002**, *340*, 133.

(25) Wood, R. M.; Palenik, G. J. *Inorg. Chem.* **1998**, *37*, 4149.

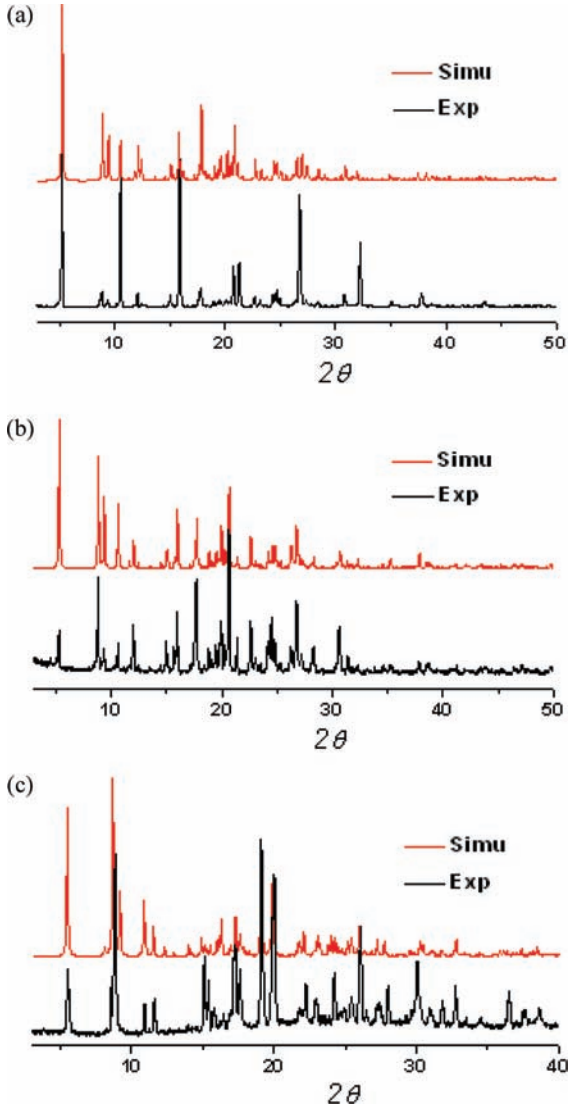

Figure 3. Simulated and experimental powder XRD patterns for (a) **1**, (b) **2**, and (c) **3**.

XRPD Results. In order to confirm the phase purity of the bulk materials, X-ray powder diffraction (XRPD) experiments have been carried out for complexes **1**−**3**. The XRPD experimental and computer-simulated patterns are shown in Figure 3. The experimental patterns of compounds **1** and **2** are in good agreement with the corresponding simulated ones, indicating the phase purity of the as-synthesized products. In the experimental pattern of **3**, although a few diffraction peaks are slightly broadened in comparison with those simulated from the single-crystal model, it still can be well considered that the bulk synthesized material and the as-grown crystals are homogeneous.

Magnetic Properties. Variable-temperature magnetic susceptibility data for **1** were collected with an applied dc field of 1.0 T in the 2−300 K temperature range and at an applied dc field of 500 G below 30 K. The χT product at 300 K has a value of 2.42 cm^3 K mol^{-1}, in agreement with that expected for two Ni^{II} ions with $S = 1$ and $g = 2.2$. As the temperature decreases, the χT product (Figure 4a) decreases slightly, indicating antiferromagnetic interactions within the Ni^{II} ions, until an increase to a maximum

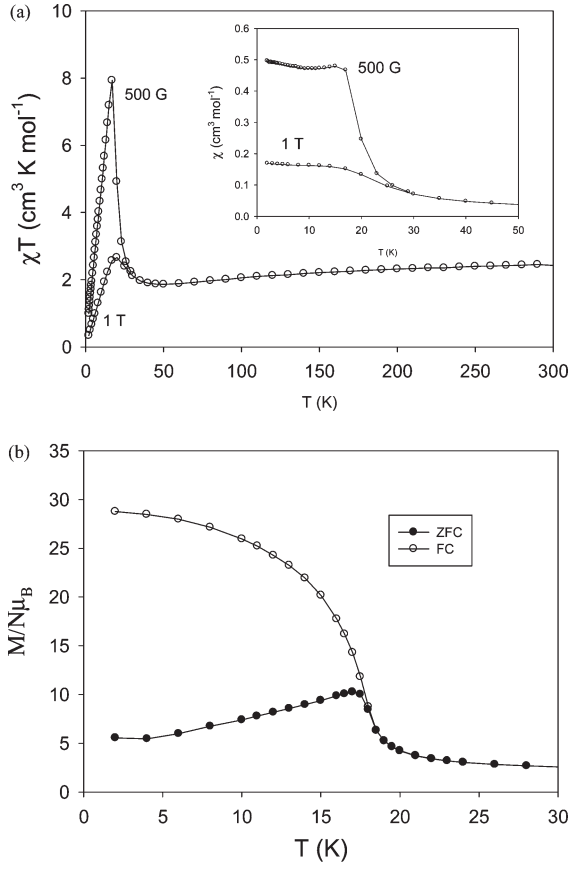

Figure 4. (a) Temperature dependence of the magnetic susceptibility for **1** at 500 G and 1 T applied fields. The inset shows the 0−50 K region. (b) ZFC-FC plot of **1** at 20 G.

at 20 K is observed. As the temperature decreases further, so does the χT product. The behavior below 30 K is strongly field-dependent. The susceptibility data suggest the onset of a weak ferromagnetic state. The divergence in the ZFC-FC plot (Figure 4b) of **1** confirms the onset of a weak ferromagnetic state at 18 K. All of these are consistent with a spin-canted antiferromagnet. A magnetization vs field plot is shown in Figure 5, in agreement with that expected for a spin-canted antiferromagnet, and there is an abrupt increase of the magnetization with field below 5000 G, and then the magnetization steadily increases linearly with the field up to a value of 0.57 at 5 T but without reaching saturation. A hysteresis loop of the magnetization vs field at 2 K is observed, as shown in Figure 6, confirming the ferromagnetically ordered state of **1** at 2 K.

The structure of **1** can be described as layers of Ni^{II} ions isolated from each other by an organic linker. Within the individual layers, the Ni^{II} ions fall into two distinct structural types, Ni1 and Ni2. The exchange interactions are of four types within the Ni1 and Ni2 ions, thus making modeling of the data not possible. The two lattices of Ni^{II} ions (Ni1 and Ni2 crystallographic types) are coupled antiferromagnetically, but the moments on each lattice are not parallel. If the N−Ni−N axes are taken as a reference, one can calculate a torsion angle of 10°. This lack of parallel alignment of the magnetic orbitals leads to a buildup of spin on the 2-D layer, perpendicular to the N−Ni−N axes, which explains

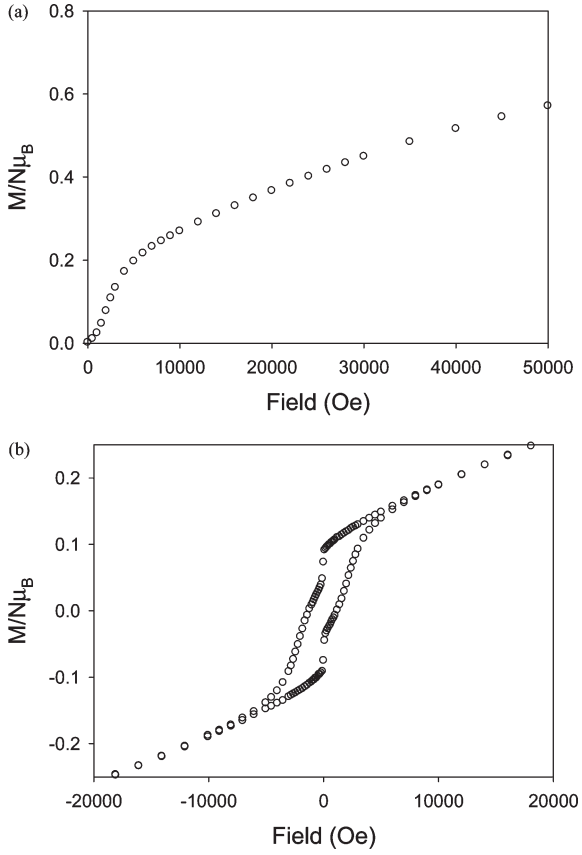

Figure 5. Field dependence of the magnetization at 2 K for **1**: (a) M vs H plot; (b) M vs H hysteresis plot.

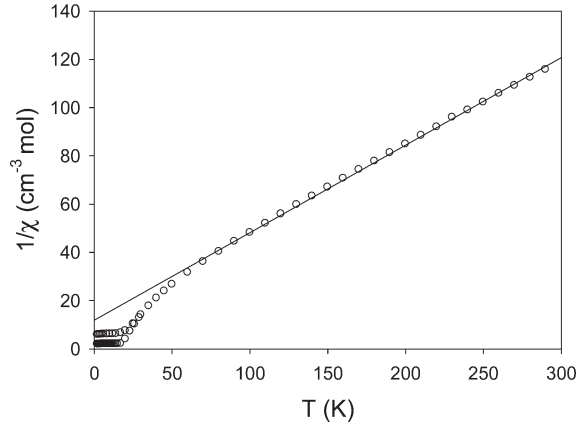

Figure 6. Curie plot for **1**. The solid line is the best fit to the Curie−Weiss law.

why the M vs field measurement resembles that of a ferromagnet but the saturation value for two Ni^{II} ions is never reached. To evaluate the magnetic exchange interactions in **1**, the susceptibility data were fitted to the Curie−Weiss law, as shown in Figure 6, and a J value was extracted using mean-field theory (MFT).[26] The fitting to the Curie−Weiss law afforded a Curie constant of $C = 2.75\ cm^3\ K\ mol^{-1}$ and a Weiss constant of $\Theta = -32.81$ K. MFT affords an average coupling constant of $J = -3.60\ cm^{-1}$.

(26) Carlin, R. L. *Magnetochemistry*; Springer: New York, 1986.

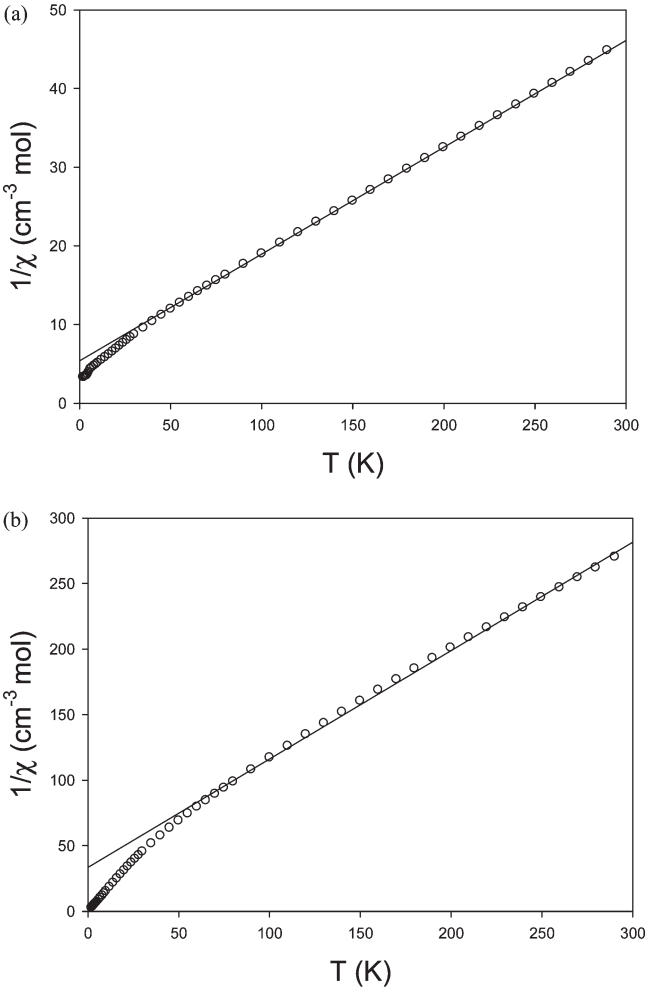

Figure 7. (a) Curie plots for (a) **2** and (b) **3**. In both cases, the solid line is the best fit to the Curie−Weiss law.

For **2** and **3**, their susceptibility data were also collected and their Curie plots are shown in parts a and b of Figure 7, respectively. The susceptibility follows the Curie−Weiss law down to 50 K. The Curie−Weiss law fitting, shown as a solid line in the plots, affords $C = 7.36\ cm^3\ K\ mol^{-1}$, $\Theta = -39.60$ K, and $J = -0.99\ cm^{-1}$ for **2** and $C = 1.20\ cm^3\ K\ mol^{-1}$, $\Theta = -40.59$ K, and $J = -11.88\ cm^{-1}$ for **3**. For the Co^{II} and Cu^{II} complexes there is no field dependence of the susceptibility. The torsion angles, defined as for compound **1** as the torsion between the N−M−N axes, are 7 and 6°, respectively, for **2** and **3**, smaller than that of **1**.

Conclusion

Three isostructural coordination polymers **1**−**3** based on the metal−formate 2D layer, which is pillared by the rodlike ligand **L**, have been synthesized under different conditions. Topological analysis indicates that these pillar-layer MOFs represent the first example of a Kagomé lattice based on the heterogeneous four-connected nodes among formate compounds. Furthermore, the formate anion of this pillar-layered structure exhibits three different bridging modes: anti-anti, syn-anti, and 3.21. This series of compounds **1**−**3** with different spin carriers provide a good system for comparative magnetic studies. Also, magnetic analyses reveal

that only the Ni^{II} compound (**1**) shows canted antiferromagnetic behavior. The preliminary results presented here greatly enrich the assembled chemistry of pillar-layer MOFs and also provide a promising pathway for new magnetic systems.

Acknowledgment. This work was supported by the 973 Program of China (No. 2007CB815305) and financial support from the Spanish Government (Grant CTQ2006/03949BQU and Ramón y Cajal contract).

Supporting Information Available: CIF files giving X-ray crystallographic data for compounds **1**−**3** and a figure giving the crystal structure of compound **4**. This material is available free of charge via the Internet at http://pubs.acs.org.